# S-nitrosylation of syntaxin 1 at Cys145 is a regulatory switch controlling Munc18-1 binding

Zoe J Palmer, Rory Duncan, James R. Johnson, Lu-Yun Lian, Luciane Vieira Mello, David Booth, Jeff W Barclay, Margaret E Graham, Robert D Burgoyne, Ian Prior, et al.

# *S*-nitrosylation of syntaxin 1 at Cys145 is a regulatory switch controlling Munc18-1 binding

[1]Zoë J. Palmer, [2]Rory R. Duncan, [1]James R. Johnson, [3]Lu-Yun Lian, [3]Luciane V. Mello, [1]David Booth, [1]Jeff W. Barclay, [1]Margaret E. Graham, [1]Robert D. Burgoyne, [1]Ian A. Prior and [1]Alan Morgan*.

[1]The Physiological Laboratory, School of Biomedical Sciences, University of Liverpool, Crown St, Liverpool, L69 3BX, UK

[2]Centre for Integrative Physiology, University of Edinburgh, Edinburgh, EH8 9XD, UK

[3]School of Biological Sciences, University of Liverpool, Crown St, Liverpool, L69 3BX, UK

*To whom correspondence should be addressed. Tel. +44 (0)151 794 5333; Fax +44 (0)151 794 5337; email: amorgan@liverpool.ac.uk

**Running title**: Syntaxin nitrosylation

**Abbreviations**: NO, nitric oxide; NEM, *N*-ethylmaleimide; NSF, NEM-sensitive fusion protein; SNAP, soluble NSF attachment protein; SNARE, SNAP receptor; SM, Sec1/Munc18-like; GST, glutathione *S*-transferase; EGFP, enhanced green fluorescent protein; EYFP, enhanced yellow fluorescent protein.

**ABSTRACT**

Exocytosis is regulated by nitric oxide (NO) in many cell types, including neurons. Here we show that syntaxin 1a is a substrate for *S*-nitrosylation and that NO disrupts the binding of Munc18-1 to the closed conformation of syntaxin 1a in vitro. In contrast, NO does not inhibit SNARE complex formation or binding of Munc18-1 to the SNARE complex. Cys145 of syntaxin 1a is the target of NO, as a non-nitrosylatable C145S mutant is resistant to NO and novel nitrosomimetic C145 mutants mimic the effect of NO on Munc18-1 binding in vitro. Furthermore, expression of nitrosomimetic syntaxin 1a in living cells affects Munc18-1 localisation and alters exocytosis release kinetics and quantal size. Molecular dynamics simulations suggest that NO regulates the syntaxin-Munc18 interaction by local rearrangement of the syntaxin linker and H3c regions. Thus, *S*-nitrosylation of Cys145 may be a molecular switch to disrupt Munc18-1 binding to the closed conformation of syntaxin 1a, thereby facilitating its engagement with the membrane fusion machinery.

**Key words**: membrane fusion/neurotransmission/nitric oxide/SM protein/SNARE

## INTRODUCTION

Exocytosis, the fusion of vesicles with the plasma membrane, can occur in a constitutive or regulated manner. In regulated exocytosis, fusion is generally triggered by an increase in the intracellular free $Ca^{2+}$ concentration, but further control is exerted by post-translational modifications to the exocytotic machinery via intracellular messengers [1]. Indeed, protein kinase C modulates $Ca^{2+}$-triggered exocytosis in virtually all secretory cells via phosphorylation of multiple substrates [2]. For example, in adrenal chromaffin cells, the early stage of vesicle recruitment and the late stage of fusion pore expansion are regulated by phosphorylation of SNAP-25 on Ser187 and Munc18-1 on Ser313, respectively [3, 4]. Nitric oxide (NO) has also been shown to modulate exocytosis in a wide range of cell types, acting variously to stimulate (e.g. in brain synaptosomes [5] and pancreatic beta cells [6]) or inhibit (e.g. in endothelial cells [7] and platelets [8]) exocytosis. Again, multiple effects of NO are evident in adrenal chromaffin cells, where NO reduces the number of vesicles undergoing fusion, but also acts on a late stage in the exocytosis process to alter the kinetics and extent of transmitter release in the remaining fusion events [9]. It seems likely, therefore, that NO acts on more than one target to achieve these varied effects on exocytosis.

The classical mechanism of action of NO is to stimulate guanylate cyclase, with the consequent increased production of cGMP leading to the activation of protein kinase G and cyclic nucleotide-gated channels [10]. However *S*-nitrosylation – the direct post-translational modification of cysteine residues in proteins by NO – is an alternative physiological function of NO [11]. Although many of the reported effects of NO on exocytosis are mediated by cGMP, others are cGMP-independent. For example, the inhibitory effect of NO on exocytosis from platelets and endothelial cells is caused by *S*-nitrosylation [7, 8]. In both cases, *S*-nitrosylation of NSF is thought to inhibit exocytosis by preventing NSF-induced SNARE complex disassembly [7, 12].

Although NSF is an important target of NO in exocytosis, it is unlikely to be the only relevant *S*-nitrosylation substrate even in cells of the cardiovascular system [13]. Furthermore, the stimulatory effects of NO in neuronal/endocrine cells are difficult to reconcile with an inhibitory action on NSF. We therefore reasoned that other components of the conserved exocytosis machinery might be substrates for *S*-nitrosylation. Here we report that *S*-nitrosylation of Cys145 in the SNARE protein, syntaxin 1a, acts as a molecular switch, turning off the Munc18-1 interaction mode that precludes SNARE complex formation, thereby facilitating interaction with the membrane fusion machinery.

## MATERIALS AND METHODS

### Materials
Unless otherwise stated, all materials were obtained from Sigma.

### Plasmids
Plasmids encoding syntaxin 1a (residues 4-285) and GST-syntaxin 1a (residues 4-266) were gifts from Dr. R. Scheller (Genentech, USA). Open (L165A/E166A) mutant versions of these plasmids have been previously described [14]. Cys145 was mutated by site directed mutagenesis in the GST-syntaxin 1a (4-266) construct for biochemical analyses and in the mCerulean-syntaxin 1a (1-288) construct [15] for live cell imaging.. For amperometry, the C145S and C145W mutations were introduced into full length wild type syntaxin 1a (1-288), which had been amplified by PCR from mouse brain cDNA and cloned into the expression vector pcDNA 3.1(-) (Invitrogen). The GST-complexin II plasmid was prepared by subcloning from pcDNA3-complexin II [16] into pGEX-4T (GE Healthcare). The pQE9-NSF plasmid encoding his-tagged NSF was a gift from Dr. J. Rothman (Columbia University, USA). Recombinant proteins were expressed and purified as previously described [14, 17, 18][19].

### Detecting *S*-nitrosylation:
#### *Biotin Loss Assays*
Rat or bovine brain homogenates prepared as described [20], were dialysed against 10mM HEPES, pH 7.4, 0.1mg/ml PMSF before an equal volume of 10mM HEPES, pH 7.4, 0.2M NaCl, 2mM EDTA, 2% Triton X-100 was added. Following rotation for 4 hours at 4$^{o}$C, the lysate was cleared by centrifugation for 1 hour, 100,000$g_{av}$, 4$^{o}$C. Protein *S*-nitrosylation was detected using the biotin loss method [21]. Briefly, brain lysate or purified recombinant protein was mixed with HEN buffer (20 mM HEPES, 1 mM EDTA, 0.1 mM neocuproine, pH 7.4), and incubated at room temperature with 1 mM GSNO or NOR-1 for 45 mins before addition of 0.5 mM biotin-HPDP or biotin-BMCC (Pierce) for 45 mins. Following SDS PAGE and transfer to nitrocellulose, biotinylated proteins were detected using avidin-HRP overlay.

#### *Affinity purification*
Biotinylated brain lysate was acetone precipitated to remove excess unbound biotin and resuspended in HEN buffer with 1% Triton X-100. Biotinylated proteins were precipitated using neutravidin beads and detected by avidin overlay and western blotting. Syntaxin 1 was immunoprecipitated from biotinylated brain lysate using the HPC-1 antibody and mouse IgG was used to control for non-specific binding. Samples were western blotted with HPC-1 antibody and subjected to avidin overlay to detect biotinylation.

### Protein Interaction studies
#### *Bead-based Binding Assays*
20 µg of GST-tagged proteins were bound to glutathione-coated beads for 1 h at 4$^{o}$C. Beads were washed with neutralisation buffer (20 mM HEPES, 100 mM NaCl, 1mM EDTA, 0.5 % Triton X-100, pH 7.7) before incubation with pre-cleared bovine brain lysate for 1 hour at 4$^{o}$C with rotation. After washing, bound proteins were eluted by boiling in SDS-PAGE sample buffer. The samples were subjected to SDS PAGE and either stained using Coomassie blue or western blotted. To investigate the effects of

NEM and NO, beads were resuspended in HEN buffer and incubated for 30 minutes at 4°C with NEM or NO donors either before or after incubation with brain lysate.

***Plate-based assay of GST- syntaxin / $^{35}$S-Munc18 binding***

This assay was performed as described previously [22]. NEM and NOR-1 were incubated with plate-bound GST-syntaxins for 30 minutes, then washed in PBS + 0.02% Triton X-100 before addition of *in vitro* translated $^{35}$S-radiolabelled Munc18-1. Binding was detected by liquid scintillation counting as described [22]. Dose responses were as above but increasing concentrations of NO donors were added to wt syntaxin, for 30 min for NOR-1 and 45 min for SIN-1. NO release was monitored using the Griess Assay Reagent System kit (Promega).

***Plate-based assay of GST- syntaxin / His-SNAP-25 binding***

These assays were as described previously [17], using 1 µg / well GST-syntaxin. To determine the effect of NEM on syntaxin, plate-bound GST-syntaxin was treated with 2 mM NEM for 30 minutes, before continuing with the standard binding assay. To determine the effect of NEM on SNAP-25, 200 nM His–tagged SNAP-25 was treated with 2 mM NEM and incubated for 30 min before adding 2 mM DTT to quench excess NEM. The treated SNAP-25 was added to the bound syntaxin and binding detected by ELISA as described [17].

**Circular Dichroism**

GST-tagged fusion proteins were thrombin cleaved to remove the GST tag. A Jasco-J810 spectropolarimeter was used for CD measurements in the far ultraviolet region, from 190 to 260 nm. Spectra were recorded at protein concentrations of approximately 0.25 mg/ml in a cuvette of 1 mm path length in a temperature-controlled cell holder at 25°C. Averaged CD signals, corrected for the buffer, were converted to mean residue weighted molar elipticity as follows [23]:

$[\theta]_{MRW} = (100 \times \theta)/Cnl$

Where: C is the protein concentration in millimolar, $\theta$ is the measured elipticity in millidegrees, n is the number of residues and l is the pathlength in cm.

**Molecular dynamics simulations**

Molecular dynamics (MD) simulations of 15 ns each were performed on three different systems. The crystal structure of syntaxin 1a (PDB code 1DN1) was used in the simulations after manually removing the Munc18-1 component. The first system consisted of the unmodified wild type syntaxin 1a structure. The second MD run replaced Cys145 with nitrosocysteine. The replacement residue was modelled in the experimentally observed side chain conformation that clashed least with neighbours, which was that seen in PDB entry 1buw. In the third MD simulation the same cysteine residue was mutated to tryptophan using Pymol (http://pymol.sourceforge.net). Pymol's inbuilt rotamer libraries [24] were used to choose the Trp rotamer clashing least with neighbouring residues and MODELLER [25] used to relieve the remaining steric clashes. The Gromacs program [26] was used for the MD calculations using a force field appropriate for proteins in water. Modifications were made to the default Gromacs dictionary to generate an *S*-nitrosocysteine residue with the help of MOPAC 7 calculations [27]. Sodium ions were added to the simulation system to compensate for the net negative charge of the

protein. The simulation was carried out in a rectangular box with a minimal distance between solute and box edge of 0.7 nm and periodic boundary conditions were used. Only the stable part of the trajectories, the last 13.5 ns of each, was used for comparison between the three systems, using the average structure during the stable portion. Superposition was carried out using UCSF Chimera software.

**Live cell imaging**

Confocal laser scanning microscopy and image analysis in Neuro2a cells was performed as described previously [15].

**Cell culture, transfection and amperometry**

Bovine adrenal chromaffin cells and HeLa cells were cultured and transfected as previously described [28]. Three independent preparations of chromaffin cells were used for each syntaxin mutant and amperometric recordings made 3-5 days after transfection, as described previously [14].

**Statistics**

Statistical analysis was performed using non-parametric Mann-Whitney tests.

## RESULTS

### *S*-nitrosylation of exocytosis proteins

Due to the labile nature of the nitrosothiol bond, *S*-nitrosylation is difficult to detect directly. However, in recent years, indirect thiol biotinylation assays have been developed to identify *S*-nitrosylated proteins [21, 29]. In order to identify components of the exocytosis machinery that may be targets for *S*-nitrosylation, we used the biotin loss technique [21]. This method is based on the selective labelling of free thiol groups on cysteine residues by biotin-HPDP; *S*-nitrosylated cysteines cannot be labelled, and so a reduced biotinylation signal after treatment with NO provides a readout of *S*-nitrosylation. Incubation of detergent-solubilized brain lysate with biotin-HPDP resulted in the incorporation of the biotin label into a large number of proteins, as detected by SDS-PAGE and subsequent avidin-HRP overlay (Fig 1A, *inputs*). Biotinylated proteins in the lysates were then affinity purified by binding to neutravidin sepharose (Fig 1A, *pull down*). In the presence of the NO donor, GSNO, the intensity of the biotinylation signal was reduced for most proteins, indicating that *S*-nitrosylation had taken place. Lysate without any treatment showed no detectable avidin-HRP labelling (Fig 1A), confirming the specificity of the detection method. To identify components of the exocytosis machinery among these *S*-nitrosylated proteins, the pull-down samples were probed using antisera to various exocytosis proteins (Fig 1B). SNAP-25 and syntaxin 1 showed reduced GSNO-dependent binding to neutravidin sepharose, indicating that these proteins are *S*-nitrosylated. In contrast, no reduction in biotinylation was seen with Munc18-1, VAMP 2 and 14-3-3, confirming that *S*-nitrosylation is selective for a subset of proteins even in crude brain extracts [30]. As SNAP-25 and syntaxin 1 form a stable complex, it was possible that these co-precipitated on the neutravidin beads and so were not independently nitrosylated. To address this, biotinylated/nitrosylated brain lysate was immunoprecipitated with a syntaxin 1 antibody. A reduction in biotinylation was evident after treatment with the NO donor, NOR-1, demonstrating that syntaxin is *S*-nitrosylated independently of SNAP-25 (Fig 1C).

### *S*-nitrosylation of syntaxin 1a inhibits Mode 1 binding to Munc18

Incubation of recombinant proteins with NO donors has previously been observed to increase formation of the SNARE complex, whilst inhibiting binding of Munc18-1 to GST-syntaxin 1a *in vitro* [31]. However, the mechanism of action of NO was entirely unclear in these experiments, as they were performed on protein mixtures and therefore the identity of the protein target(s) of NO was impossible to determine. Since we had identified syntaxin 1, but not Munc18-1, as a target for *S*-nitrosylation, this suggested that these reported effects might be mediated by *S*-nitrosylation of syntaxin 1a. To test this, the same GST-syntaxin 1a construct used in the earlier study (encoding cytoplasmic domain residues 4-266) was pre-treated with NOR-1 or N-ethylmaleimide (NEM) before being incubated with untreated brain lysate, to ensure that these drugs could only act on syntaxin 1a (Fig 2A, *pre-assembly*). The sulfhydryl alkylating agent, NEM, was included as it was previously shown to mimic the effect of NO in inhibiting Munc18-1 binding to syntaxin 1a [31] and has the advantage of causing irreversible thiol modification, unlike NO. Both NOR-1 and NEM inhibited Munc18-1 binding to GST-syntaxin 1a, as visualised by reduced levels of an approximately 67 kDa band in Coomassie blue-stained gels (Fig 2A). This band was excised and analysed by mass spectrometry and confirmed to be Munc18-1 (data not shown).

The binding of Munc18-1 to the GST-syntaxin 1a (4-266) construct in this assay is likely to occur mainly through the classical (Mode 1) binding to the closed conformation of syntaxin [32, 33], as it is strongly inhibited by mutations that favour a more 'open' conformation [14]. In order for syntaxin 1 to bind to the other SNAREs and execute fusion, this inhibitory interaction must be dissociated to allow syntaxin to shift into an open conformation, although it is unclear what regulates this process. Therefore we investigated if NO could disrupt (post assembly) as well as inhibit (pre assembly) the Munc18-1/ syntaxin 1 interaction. Recombinant GST-syntaxin 1a was incubated with bovine brain extract and then treated with NOR-1 or NEM. Both treatments resulted in disruption of Munc18-1 binding to syntaxin (Fig 2A, *post assembly*). NEM treatment resulted in less binding in both pre- and post-assembly protocols, which may be explained by the transient and irreversible cysteine modifications caused by *S*-nitrosylation and NEM, respectively. To test if this Munc18-1 dissociation would facilitate syntaxin 1 binding to the other SNAREs, samples were western blotted using antisera to SNAP-25 and VAMP 2. Treatments with both NOR-1 and NEM resulted in an increase in SNAP-25 and VAMP binding to syntaxin, which mirrored the reduction in Munc18-1 binding (Fig 2B).

To quantify these effects and to confirm that they were due solely to modification of syntaxin, recombinant protein binding assays using coated 96-well plates were performed. NOR-1 and NEM inhibited binding of *in vitro* translated $^{35}$S-labelled Munc18-1 to GST-syntaxin 1a [22] by approximately 50% and 75%, respectively (Fig 2C), consistent with the pull-down experiments. In contrast, the binding of purified his-tagged SNAP-25 to GST-syntaxin 1a [17] was unaffected by NEM treatment of syntaxin (Fig 2D). This suggested that the increased SNAP-25 binding caused by NEM in the pull down experiments from a complex mix of proteins was indirectly due to Munc18-1 dissociation from syntaxin 1, rather than a direct increase in affinity for SNAP-25. As SNAP-25 had also been identified as a potential target for nitrosylation, the same assay was used to investigate if treating SNAP-25 with NEM affected the syntaxin 1/SNAP-25 interaction (Fig 2D). To do this, NEM was pre-incubated with recombinant SNAP-25 and then quenched with DTT before adding the SNAP-25 to GST-syntaxin 1a. This had no effect on the binding between SNAP-25 and syntaxin, therefore all subsequent work focussed on investigating syntaxin modification. To determine the concentration-dependence of the inhibitory effect of NO on the Mode 1 Munc18-1/syntaxin 1a interaction, binding assays were performed using a range of concentrations of structurally distinct NO donors, NOR-1 and SIN-1 (Fig 2E). Griess assays were performed in parallel to measure the amount of NO released by each concentration of NO donor during the incubations. NOR-1 and SIN-1 caused similar dose-dependent inhibition of Munc18-1 binding at equivalent released NO concentrations (Fig 2E). This inhibition was saturable with NOR-1, yielding an $IC_{50}$ value of 1.1 ± 0.9 µM NO.

**Binding of Munc18-1 to the SNARE complex is not inhibited by NO**

In addition to the classical Mode 1 binding to the closed conformation of syntaxin, Munc18-1 can also bind to the extreme N-terminus of syntaxin (Mode 2), which enables its Mode 3 binding to the SNARE complex [15, 34-38]. As N-terminal truncation [15] and tagging [35] of syntaxin interferes with Mode 2/3 binding, the GST-syntaxin 1a (4-266) construct could not be used to determine the effect of NO/NEM on Munc18-1 binding to the SNARE complex. Instead, we used an affinity purification approach using GST-complexin [18]. Consistent with the selective binding of complexin to the SNARE complex [39], syntaxin 1 and VAMP 2 were

readily detected in pull downs from brain lysate using GST-complexin, but not in GST controls (Fig 3A). The recovery of SNARE complexes was unaffected by treatment with NEM, reinforcing our finding that the syntaxin/SNAP-25 interaction is insensitive to this treatment. In contrast, the co-association of native Munc18-1 with the SNARE complex was strongly inhibited by NEM (Fig 3A). In this experiment, NEM was applied to the whole protein mixture, so it was not possible to determine if the drug acted at the level of the SNARE complex, Munc18-1 or both. To address this issue and to determine whether NO would have the same effect, a 2-stage incubation protocol was adopted. In stage 1, all samples were incubated with brain lysate, either untreated or in the presence of NOR-3 or NEM. After washing, samples were either eluted or alternatively subjected to a second incubation with brain lysate in the presence or absence of NOR-3 or NEM (Stage 2). NEM treatment of the assembled complex in either stage inhibited Munc18-1 binding (Fig 3B, compare lane 1 control with lanes 2 and 4), consistent with Fig 3A. Interestingly, selective pre-treatment of this assembled complex did not prevent the subsequent binding of Munc18-1 from untreated brain lysate (Fig 3B, lane 6), indicating that the inhibitory action of NEM on Mode 3 binding acts at the level of Munc18-1 modification. In contrast, NOR-3 treatment had no effect on Munc18-1 binding to the SNARE complex, in keeping with the apparent resistance of Munc18-1 to *S*-nitrosylation (Fig 1).

**Model of NO action on syntaxin 1a: modification of Cys145**

Syntaxin 1a has only one cysteine residue in its cytoplasmic domain, Cys145, which is located toward the C-terminal end of the Hc helix. This cysteine is evolutionarily conserved in neuronal syntaxins (syntaxin 1a/b homologues) across a wide variety of organisms, but is absent from most non-neuronal homologues (Fig 4A). In the crystal structure of Munc18-1 bound via Mode 1 to the closed conformation of syntaxin 1a [40], Cys145 makes no contacts with Munc18-1. Instead, Cys145 interacts with Ile202 in the H3 domain (the SNARE motif) of syntaxin 1a (Fig 4B, top panels). Therefore, the inhibition of Mode 1 binding by NO/NEM modification of syntaxin observed here is unlikely to be due to direct occlusion of a Munc18-1 binding site. Rather, modification of this Cys145 is more likely to act allosterically, inducing a conformational change in syntaxin that indirectly affects Munc18-1 binding.

To investigate the potential structural consequences of *S*-nitrosylation of Cys145, we performed molecular dynamics simulations of wild type and *S*-nitroso-cysteine modified syntaxin 1a, using atomic coordinates from the 1dn1 crystal structure. The average stable structures achieved over the last 13.5 nanoseconds of 15-nanosecond simulations revealed little change to the Ha, Hb and Hc helices, with the two structures being basically super-imposable in these regions (Fig 4B, bottom left). However, Cys145 *S*-nitrosylation affected the local structure of syntaxin C-terminal to this residue, resulting in movement of the linker region that connects Hc to the H3 SNARE helix, and also alterations in the orientation of the C-terminal end of the SNARE motif itself. Disruption of the Cys145-Ile202 hydrophobic interaction by *S*-nitrosylation in the simulation destabilised the association of the H3a helix of the SNARE motif with the Hc helix, which in turn prevented Leu169 in the linker from making its normal contact with His199 in the H3a helix, thus reorienting the linker domain. Interestingly, mutations in the linker domain are used to create the 'open' syntaxin mutant, which exhibits reduced Mode 1 Munc18-1 binding [32]. In addition, the *S*-nitrosylation-induced repositioning of the H3c subdomain, a 5-residue helix near the C-terminus that makes multiple contacts with the central cavity of Munc18-1,

would have profound effects on Mode 1 Munc18-1 binding, as mutation of a single residue in the H3c helix, Ile233, strongly inhibits this interaction [14].

**Effects of mutating Cys145 on syntaxin structure and function *in vitro***

To analyse the effects of Cys145-specific modification on syntaxin, we set out to create mutant proteins that would mimic or be resistant to *S*-nitrosylation (analogous to the phosphomimetic and non-phosphorylatable mutants used in protein phosphorylation studies). Cys-Ser substitutions are commonly used to create non-*S*-nitrosylatable proteins [11]. Furthermore, syntaxins 2 and 3 both contain a serine residue at position 145 in an otherwise highly conserved region (Fig 4A), so it was assumed that a C145S mutation would not affect the overall structure or function of syntaxin 1a. In contrast, 'nitrosomimetic' mutants have no precedence within the literature. We therefore generated mutations that might approximate an *S*-nitrosylated cysteine residue, using substitutions to methionine and tryptophan (C145M, C145W). Methionine was chosen as it preserves the sulphur atom of cysteine, but replaces the attached hydrogen with a methyl group, which may resemble an NO group attached to the sulphur. However, as this methyl group is still less bulky than NO, we also used a tryptophan substitution, reasoning that this large aromatic amino acid may more effectively mimic modification by NO and NEM. Molecular dynamics simulations of the C145W mutant revealed structural alterations to the linker region and destabilisation of the H3c helix (Fig 4B, bottom right), the same regions altered in the Cys145-*S*-nitrosylated simulation, suggesting that C145W might be a suitable nitrosomimetic mutant. Therefore, these Cys145 mutations were introduced into GST-syntaxin 1a (4-266) to enable biochemical analysis of the mutant proteins.

If Cys145 is the sole nitrosylation site in the protein, then mutation of this residue to any other amino acid should inhibit biotin-HPDP labelling in the biotin loss assay. To test this, wild type and C145W mutant GST-syntaxin 1a were purified and then their GST tags were removed by thrombin cleavage. These were then used in the biotin loss assay, along with purified recombinant his-tagged NSF as a positive control (Fig 5A). Wild type recombinant syntaxin exhibited robust biotinylation that was reduced by NO treatment, similar to that seen for the native brain protein (Fig 1). NSF also showed clear NO-inhibited biotinylation, thus further confirming the validity of the biotin loss assay. In contrast, biotinylation of C145W syntaxin was barely detectable (Fig 5A). Therefore, Cys145 is indeed an *S*-nitrosylation site, at least in vitro.

We also investigated the effect of Cys145 mutations on Mode 1 Munc18-1 binding (Fig 5B). The C145S mutant bound Munc18-1 to the same extent as wild type syntaxin 1a, but was unaffected by NOR-1 and NEM. This confirmed that the inhibitory effect of these drugs on Munc18-1 binding was entirely mediated via modification of syntaxin 1a at Cys145, consistent with the biotin loss assay in Fig 5A. The C145M and C145W mutants exhibited reduced Munc18-1 binding, similar to the inhibition of wild type syntaxin by NOR-1 and NEM, respectively (Fig 5B). This further supports the idea that *S*-nitrosylation of Cys145 regulates Mode 1 Munc18-1 binding and suggests that these mutants may indeed represent nitrosomimetic versions of syntaxin. The reduction in Munc18-1 binding by C145W in this pull down assay was similar to that seen when the 'open' (Fig 5B) and I233A mutations (data not shown) were introduced into the same GST-syntaxin 1a (4-266) construct. In order to quantify Munc18-1 binding, assays were performed using GST-tagged syntaxins bound to glutathione-coated plates and incubated with $^{35}$S-labelled *in vitro* translated Munc18 (Fig 5C). This revealed a 62 % and 87 % reduction in Munc18-1 binding to

C145M and C145W, respectively; similar to the inhibition of binding seen with NOR-1 and NEM (60% and 80%, respectively). As no inhibition of Munc18-1 binding was seen with the C145S mutant, this effect is specific to nitrosomimetic residues and not simply a consequence of mutating Cys145. All mutants exhibited similar levels of SNAP-25 binding (Fig 5D), consistent with the observation (Fig 2) that NEM does not affect this interaction. The finding that SNAP-25 binding was normal in the nitrosomimetic mutants suggested that the observed reduction in Munc18-1 binding was unlikely to be due to gross conformational defects in the recombinant mutant proteins. However, to directly test this, the proteins were analysed by circular dichroism spectroscopy after removal of their GST tags. Wild type, C145M and C145W proteins exhibited super-imposable spectra, confirming that there were no major changes in the structural integrity of the nitrosomimetic mutants (Fig 5E).

**Effect of syntaxin 1a Cys145 mutants on Munc18-1 interaction in living cells**

To investigate the relevance of Cys145 for Munc18-1 binding in a cellular context, we introduced non-nitrosylatable (C145S) and nitrosomimetic (C145W) mutations into mCerulean-tagged full length syntaxin 1a (residues 1-288). These were then co-transfected with EYFP-tagged Munc18-1 in Neuroblastoma 2A (N2A) cells and visualised by fluorescence microscopy (Fig 6A). Wild type syntaxin 1a co-localised with Munc18-1 at the plasma membrane and also at perinuclear areas, as previously shown [15]. The C145S mutant had an identical distribution, consistent with the similar behaviour of this mutant to wild type syntaxin 1a in all *in vitro* binding assays. In contrast, diffuse cytoplasmic staining of Munc18-1 was evident upon co-expression of the C145W nitrosomimetic mutant and treatment of wild type syntaxin 1a with NEM (note red hue in merged panels). Strikingly, this effect of NEM was completely abolished in the C145S mutant (Fig 6A), indicating that the inhibition of syntaxin 1a/Munc18-1 colocalization by NEM is absolutely dependent on Cys145 modification. In order to quantify the colocalization of Munc18-1 with syntaxin in the whole cell, rather than in a single confocal slice, the intensity for each channel in each voxel was determined (shown in the 2-D histogram panel, with a colour scale representing frequency). The residual map displays weighted residuals from the line fit to the histogram, thus indicating fluorescence channel covariance. The diffuse cytoplasmic purple hue evident in the NEM-treated wild type $Syx_{1\text{-}288}$ and the C145W samples corresponds to regions where EYFP-Munc18-1 is not co-variant with mCerulean-syntaxin fluorescence. Analysis of these data from multiple cells revealed a significant decrease in the correlation coefficient for NEM-treated wild type $Syx_{1\text{-}288}$ and C145W-expressing cells, but no effect of NEM on C145S-transfected cells (Fig 6B).

It was notable that significant plasma membrane staining of Munc18-1 remained in C145W-expressing cells, but not in NEM-treated wild type-expressing cells. To determine if this residual Munc18-1 was actually interacting with the C145W protein, we used fluorescence lifetime imaging (FLIM). A single fluorescence lifetime of the donor, mCerulean-$Syx_{1\text{-}288}$, was observed in the absence of an energy acceptor (Figure 7A; *top right panel*), with a mean value of 2288 ± 40 ps. When co-expressed with the EYFP-Munc18-1 Förster resonance energy transfer (FRET) acceptor, a reduction in the mean mCerulean-$Syx_{1\text{-}288}$ donor fluorescence lifetime occurred, consistent with FRET due to interaction of the two tagged proteins [15]. This is visualised in the FLIM map as yellow/green staining, as opposed to the blue hue with $Syx_{1\text{-}288}$ alone (quantified in Fig 7B). Treatment of $Syx_{1\text{-}288}$ with NEM abolished detectable interaction with Munc18-1 on the cell surface, as indicated by

the loss of the short fluorescence lifetime (note blue plasma membrane staining, similar to that seen in the absence of Munc18-1). In contrast, identical NEM treatment of $Syx_{1-288}$ [C145S] did not abolish its interaction with Munc18-1 at the plasma membrane. Similarly, Munc18-1 interaction at the cell surface was preserved in the $Syx_{1-288}$ [C145W] nitrosomimetic mutant. These data suggest that the Mode 1 binding of Munc18-1 to syntaxin 1a is not essential for interaction at the plasma membrane. The abolition of this interaction by NEM likely reflects its inhibitory action on multiple binding Modes via effects on both syntaxin 1a and Munc18-1, as seen in our *in vitro* binding assays (Fig 3). Consistent with this need to act on both proteins, NEM does not abolish plasma membrane interaction when syntaxin 1a cannot be modified (C145S).

**Effect of syntaxin 1a Cys145 mutants on exocytosis**

In adrenal chromaffin cells, overexpression of syntaxin mutants defective in Mode 1 Munc18-1 binding alters single vesicle release kinetics, but has no effect on the frequency of exocytosis events [14]. As nitrosomimetic (but not non-nitrosylatable) Cys145 mutants exhibit impaired Mode 1 binding, we investigated the effect of Cys145 modification on exocytosis. To do this, chromaffin cells were co-transfected with syntaxin mutants and EGFP as a reporter and exocytosis analysed by amperometry. Overexpression of syntaxin mutants had no significant effect on the frequency of exocytotic events, with similar amperometric traces being recorded from control and transfected cells (supplementary Fig 1). When individual amperometric spikes (corresponding to single exocytotic release events) were analysed, C145S transfected cells were similar to untransfected cells in all kinetic parameters (Fig 8A). However, C145W overexpression resulted in increased rise and fall times, half-width and quantal size, as did overexpression of open syntaxin used as a control (Fig 8A). As C145W and C145S differ only in the nature of the Cys145 mutation, this indicates a nitrosomimetic-residue-specific effect of the mutant on exocytosis, consistent with the Munc18-1 binding data. In addition, as there was no difference between the mutants in protein expression level (Fig 8B; performed in HeLa cells due to the low transfection efficiency of chromaffin cells), these effects are not due to differential stability of the mutant proteins. Therefore, overexpression of C145W mutant syntaxin increases quantal size and slows the kinetics of individual exocytotic fusion events, consistent with the impaired Mode 1 Munc18-1 binding characteristics of this nitrosomimetic mutant.

**Discussion**

*S*-nitrosylation has emerged as an important mechanism by which NO modulates various physiological processes, including exocytosis. However, identification of the relevant substrates has been hampered by the technical difficulty of detecting *S*-nitrosylated proteins within cellular extracts. The development of indirect thiol biotinylation assays in recent years [21, 29] has facilitated identification of a number of potential targets, but very few examples exist where the molecular mechanism by which site-specific S-nitrosylation regulates protein structure and function is understood. Here we have used the biotin loss technique to demonstrate specific NO-induced *S*-nitrosylation of both endogenous syntaxin 1 from brain extracts and recombinant syntaxin 1a, consistent with findings using purified vesicle preparations [21]. Importantly, syntaxin 1 has been shown to be endogenously *S*-nitrosylated in rat brain *in vivo* in the absence of NO donors, indicating that this modification occurs physiologically [41]. Using a combination of biochemical, cellular and molecular modelling approaches we have shown that modification of the sole *S*-nitrosylation site in the cytoplasmic domain of syntaxin 1a, Cys145, specifically inhibits the classical mode of Munc18-1 binding. Our development of a novel nitrosomimetic mutant approach – analogous to the phosphomimetic mutants that underpin many protein phosphorylation studies – was particularly important here, and may be of more general use to study the effect of site-specific *S*-nitrosylation in vivo.

Although a 'consensus sequence' for *S*-nitrosylation is difficult to define, *S*-nitrosocysteines are typically located within areas of positive charge and are often close to aromatic amino acids in buried regions [30]. The sequence surrounding Cys145 in syntaxin 1a fits these criteria and is highly conserved (YRXRCK) in all neuronal syntaxins throughout evolution (Fig. 4A). Interestingly, the syntaxin family as a whole is relatively cysteine-poor, for example syntaxin 3 contains no cysteines. The retention of a single cysteine residue in the cytoplasmic domain of syntaxin 1a in various species suggests a specific function; potentially regulation by *S*-nitrosylation, or by other modifications such as oxidation, glutathionylation or palmitoylation. It is interesting to note that, although generally absent from non-neuronal syntaxins, the Cys145-homologous residue is also found in syntaxins 11 and 19. Little is known about the function of syntaxin 19, but syntaxin 11 is involved in regulated exocytosis in cytotoxic lymphocytes [42]. As syntaxin 4 also contains a cysteine residue in its Hc domain (albeit 11 residues upstream of the Cys145-homologous residue in syntaxin 1a, see Fig 4A), and is involved in regulated exocytosis in various cell types, it is tempting to speculate that cysteine modification may be a specific regulatory mechanism for syntaxins involved in regulated exocytosis.

Recently, our understanding of Munc18-1 function has been dramatically illuminated by the discovery that, in addition to its originally discovered (Mode 1) interaction with the closed conformation of syntaxin 1 [33], Munc18-1 can also bind to an N-terminal peptide of syntaxin 1a (Mode2) [15]. This Mode 2 interaction is essential for Munc18-1 binding to the SNARE complex (Mode 3) [35], which facilitates membrane fusion [34]. Although Mode 2 and 3 interactions are common to diverse SM/syntaxin pairs, the Mode 1 interaction has, to date, only been documented in homologues involved in regulated exocytosis, including mammalian Munc18-1 and Munc18c, and *C. elegans* UNC-18 [37][38][43]. Disruption of the Mode 1 interaction via transition to the open conformation of UNC-64 (*C. elegans* syntaxin 1) has been suggested to be part of the priming process that leads to synaptic vesicle docking and fusion *in vivo* [44, 45]. Our finding that *S*-nitrosylation of syntaxin 1a at Cys145 specifically antagonises Mode 1 binding suggests that post-translational

modification of this cysteine residue could be a mechanism to regulate this potentially inhibitory interaction, thereby facilitating the interaction of syntaxin with cognate SNAREs, and subsequently Munc18-1 in the Mode 2/3 interaction, to execute membrane fusion. Alternatively, as Mode 1 binding of Munc18-1 to the closed conformation of syntaxin has recently been shown to play a positive role in Rab3-dependent vesicle docking [18, 46, 47], *S*-nitrosylation of syntaxin could potentially also act as an inhibitory regulator of this early stage of the exocytosis process in some cell types. Polyunsaturated fatty acids (PUFAs) have recently been shown to inhibit Mode 1 binding, but by a distinct mechanism involving a major conformational change detectable by CD spectroscopy, which likely results in syntaxin assuming a more open conformation [48]. Interestingly, PUFA supplementation increased *S*-nitrosylation of endogenous syntaxin 1 in rat hippocampus *in vivo* [41], suggesting that opening of syntaxin via PUFAs may increase the probability of Cys145 modification, providing a potential synergistic link between these two regulatory mechanisms.

Analysis of exocytosis by amperometry in adrenal chromaffin cells treated with NO donors reveals two distinct effects: an overall inhibition of exocytosis and a slowing of the release kinetics and increased quantal size in the remaining individual fusion events [9]. Intriguingly, overexpression of the C145W nitrosomimetic syntaxin 1a mutant similarly slows release kinetics and increases quantal size. This suggests a potential link between NO and syntaxin in exocytosis via *S*-nitrosylation of Cys145. Such a regulatory mechanism may help to rationalise the confusing literature on the effects of NO on exocytosis, where both stimulatory and inhibitory actions are commonly reported, even in the same cell type. *S*-nitrosylation of NSF, and the consequent depletion of free SNAREs able to engage in fusion, is likely to be important for the inhibitory effects of NO [13]. However, it is difficult to see how NSF inhibition could explain the stimulation of synaptic vesicle and insulin granule exocytosis by NO [5][6] or the effect on release kinetics in chromaffin cells [9]. We suggest that *S*-nitrosylation of syntaxin at Cys145 may be a mechanism by which NO can cause such positive effects, by switching off Mode 1 Munc18-1 binding, thereby facilitating syntaxin 1 engagement with the fusion machinery. It is tempting to speculate that this may contribute to the role of NO as a retrograde messenger in synaptic plasticity [10], with post-synaptically generated NO acting locally at the presynaptic active zone to relieve the constraint of Mode 1 Munc18-1 binding, thus increasing the release probability of subsequent stimuli.

In summary, our data provide a novel molecular mechanism for switching between distinct syntaxin/Munc18 binding modes: *S*-nitrosylation of Cys145 in syntaxin 1a. Several distinct lines of evidence support this model, ranging from in silico molecular modelling, through in vitro protein-protein interaction assays, to cellular studies of protein interactions and exocytosis. Two key questions arise from this study: is this regulatory mechanism physiologically important in vivo, and is it restricted to the syntaxin 1/Munc18-1 SM pairing? Further work capitalising on the conserved nature of Cys145 in genetically tractable model organisms (Fig 4) is required to address these issues rigorously. The use of the nitrosomimetic mutant approach described here may facilitate such future studies into the role of site-specific *S*-nitrosylation on syntaxin function in vivo.

**Acknowledgements**

We thank Colin Rickman for experimental assistance and for helpful comments. This work was supported by research grants from BBSRC and the Wellcome Trust. ZP and DB were supported by MRC studentships.

## References


1 Turner, K. M., Burgoyne, R. D. and Morgan, A. (1999) Protein phosphorylation and the regulation of synaptic membrane traffic. Trends Neurosci. **22**, 459-464

2 Morgan, A., Burgoyne, R. D., Barclay, J. W., Craig, T. J., Prescott, G. R., Ciufo, L. F., Evans, G. J. and Graham, M. E. (2005) Regulation of exocytosis by protein kinase C. Biochem. Soc. Trans. **33**, 1341-4

3 Nagy, G., Matti, U., Nehring, R. B., Binz, T., Rettig, J., Neher, E. and Sorensen, J. B. (2002) Protein kinase C-dependent phosphorylation of synaptosome-associated protein of 25 kDa at $Ser^{187}$ potentiates vesicle recruitment. J. Neurosci. **22**, 9278-9286

4 Barclay, J. W., Craig, T. J., Fisher, R. J., Ciufo, L. F., Evans, G. J. O., Morgan, A. and Burgoyne, R. D. (2003) Phosphorylation of Munc18 by Protein Kinase C Regulates the Kinetics of Exocytosis. J. Biol. Chem. **278**, 10538-10545

5 Meffert, M. K., Premack, B. A. and Schulman, H. (1994) Nitric oxide stimulates Ca(2+)-independent synaptic vesicle release. Neuron **12**, 1235-44

6 Smukler, S. R., Tang, L., Wheeler, M. B. and Salapatek, A. M. (2002) Exogenous nitric oxide and endogenous glucose-stimulated beta-cell nitric oxide augment insulin release. Diabetes **51**, 3450-60

7 Matsushita, K., Morrell, C. N., Cambien, B., Yang, S. X., Yamakuchi, M., Bao, C., Hara, M. R., Quick, R. A., Cao, W., O'Rourke, B., Lowenstein, J. M., Pevsner, J., Wagner, D. D. and Lowenstein, C. J. (2003) Nitric oxide regulates exocytosis by S-nitrosylation of N-ethylmaleimide-sensitive factor. Cell **115**, 139-50

8 Morrell, C. N., Matsushita, K., Chiles, K., Scharpf, R. B., Yamakuchi, M., Mason, R. J., Bergmeier, W., Mankowski, J. L., Baldwin, W. M., 3rd, Faraday, N. and Lowenstein, C. J. (2005) Regulation of platelet granule exocytosis by S-nitrosylation. Proc. Natl. Acad. Sci. U S A **102**, 3782-7

9 Machado, J. D., Segura, F., Brioso, M. A. and Borges, R. (2000) Nitric oxide modulates a late step of exocytosis. J. Biol. Chem. **275**, 20274-9

10 Garthwaite, J. (2005) Dynamics of cellular NO-cGMP signaling. Front. Biosci. **10**, 1868-80

11 Hess, D. T., Matsumoto, A., Kim, S. O., Marshall, H. E. and Stamler, J. S. (2005) Protein S-nitrosylation: purview and parameters. Nat. Rev. Mol. Cell Biol. **6**, 150-66

12 Morgan, A. and Burgoyne, R. D. (2004) Membrane traffic: controlling membrane fusion by modifying NSF. Curr. Biol. **14**, R968-70

13 Lowenstein, C. J. (2007) Nitric oxide regulation of protein trafficking in the cardiovascular system. Cardiovasc. Res. **75**, 240-6

14 Graham, M. E., Barclay, J. W. and Burgoyne, R. D. (2004) Syntaxin/Munc18 interactions in the late events during vesicle fusion and release in exocytosis. J. Biol. Chem. **279**, 32751-60

15 Rickman, C., Medine, C. N., Bergmann, A. and Duncan, R. R. (2007) Functionally and spatially distinct modes of munc18-syntaxin 1 interaction. J. Biol. Chem. **282**, 12097-103

16 Archer, D. A., Graham, M. E. and Burgoyne, R. D. (2002) Complexin Regulates the Closure of the Fusion Pore during Regulated Vesicle Exocytosis. J. Biol. Chem. **277**, 18249-18252

17 Yang, Y., Craig, T. J., Chen, X., Ciufo, L. F., Takahashi, M., Morgan, A. and Gillis, K. D. (2007) Phosphomimetic mutation of Ser-187 of SNAP-25 increases both syntaxin binding and highly Ca2+-sensitive exocytosis. J. Gen. Physiol. **129**, 233-44

18 Graham, M. E., Handley, M. T., Barclay, J. W., Ciufo, L. F., Barrow, S. L., Morgan, A. and Burgoyne, R. D. (2008) A gain-of-function mutant of Munc18-1 stimulates secretory granule recruitment and exocytosis and reveals a direct interaction of Munc18-1 with Rab3. Biochem. J. **409**, 407-16

19 Morgan, A., Dimaline, R. and Burgoyne, R. D. (1994) The ATPase activity of N-Ethylmaleimide-sensitive fusion protein (NSF) is regulated by soluble NSF attachment proteins. J. Biol. Chem. **269**, 29347-29350

20 Sollner, T., Whiteheart, S. W., Brunner, M., Erdjument-Bromage, H., Geromanos, S., Tempst, P. and Rothman, J. E. (1993) SNAP receptors implicated in vesicle targeting and fusion. Nature **362**, 318-324

21 Prior, I. A. and Clague, M. J. (2000) Detection of thiol modification following generation of reactive nitrogen species: analysis of synaptic vesicle proteins. Biochim. Biophys. Acta **1475**, 281-6

22 Craig, T. J., Ciufo, L. F. and Morgan, A. (2004) A protein-protein binding assay using coated microtitre plates: increased throughput, reproducibility and speed compared to bead-based assays. J. Biochem. Biophys. Methods **60**, 49-60

23 Luo, P. and Baldwin, R. L. (1997) Mechanism of helix induction by trifluoroethanol: a framework for extrapolating the helix-forming properties of peptides from trifluoroethanol/water mixtures back to water. Biochemistry **36**, 8413-21

24 Dunbrack, R. L., Jr. and Cohen, F. E. (1997) Bayesian statistical analysis of protein side-chain rotamer preferences. Protein Sci. **6**, 1661-81

25 Sali, A. and Blundell, T. L. (1993) Comparative protein modelling by satisfaction of spatial restraints. J. Mol. Biol. **234**, 779-815

26 Van Der Spoel, D., Lindahl, E., Hess, B., Groenhof, G., Mark, A. E. and Berendsen, H. J. (2005) GROMACS: fast, flexible, and free. J. Comput. Chem. **26**, 1701-18

27 Stewart, J. J. (1990) MOPAC: a semiempirical molecular orbital program. J. Comput. Aided Mol. Des. **4**, 1-105

28 Evans, G. J. O., Wilkinson, M. C., Graham, M. E., Turner, K. M., Chamberlain, L. H., Burgoyne, R. D. and Morgan, A. (2001) Phosphorylation of cysteine string protein by protein kinase A: implications for the modulation of exocytosis. J. Biol. Chem. **276**, 47877-47885

29 Jaffrey, S. R., Erdjument-Bromage, H., Ferris, C. D., Tempst, P. and Snyder, S. H. (2001) Protein S-nitrosylation: a physiological signal for neuronal nitric oxide. Nat. Cell Biol. **3**, 193-7

30 Hao, G., Derakhshan, B., Shi, L., Campagne, F. and Gross, S. S. (2006) SNOSID, a proteomic method for identification of cysteine S-nitrosylation sites in complex protein mixtures. Proc. Natl. Acad. Sci. U S A **103**, 1012-7

31 Meffert, M. K., Calakos, N. C., Scheller, R. H. and Schulman, H. (1996) Nitric oxide modulates synaptic vesicle docking/fusion reactions. Neuron **16**, 1229-1236

32 Dulubova, I., Sugita, S., Hill, S., Hosaka, M., Fernandez, I., Sudhof, T. C. and Rizo, J. (1999) A conformational switch in syntaxin during exocytosis: role of munc18. EMBO J. **18**, 4372-4382

33 Yang, B., Steegmaier, M., Gonzalez, L. C. and Scheller, R. H. (2000) nSec1 binds a closed conformation of syntaxin1A. J. Cell Biol. **148**, 247-252

34 Shen, J., Tareste, D. C., Paumet, F., Rothman, J. E. and Melia, T. J. (2007) Selective activation of cognate SNAREpins by Sec1/Munc18 proteins. Cell **128**, 183-95

35 Dulubova, I., Khvotchev, M., Liu, S., Huryeva, I., Sudhof, T. C. and Rizo, J. (2007) Munc18-1 binds directly to the neuronal SNARE complex. Proc. Natl. Acad. Sci. U S A **104**, 2697-702

36 Zilly, F. E., Sorensen, J. B., Jahn, R. and Lang, T. (2006) Munc18-bound syntaxin readily forms SNARE complexes with synaptobrevin in native plasma membranes. PLoS Biol. **4**, e330

37 Burgoyne, R. D. and Morgan, A. (2007) Membrane trafficking: three steps to fusion. Curr. Biol. **17**, R255-8

38 Toonen, R. F. and Verhage, M. (2007) Munc18-1 in secretion: lonely Munc joins SNARE team and takes control. Trends Neurosci. **30**, 564-72

39 McMahon, H. T., Missler, M., Li, C. and Südhof, T. C. (1995) Complexins: cytosolic proteins that regulate SNAP receptor function. Cell. **83**, 111-119

40 Misura, K. M. S., Scheller, R. H. and Weis, W. I. (2000) Three-dimensional structure of the neuronal-Sec1-syntaxin1a complex. Nature **404**, 355-362

41 Pongrac, J. L., Slack, P. J. and Innis, S. M. (2007) Dietary Polyunsaturated Fat that Is Low in (n-3) and High in (n-6) Fatty Acids Alters the SNARE Protein Complex and Nitrosylation in Rat Hippocampus. J. Nutr. **137**, 1852-6

42 Bryceson, Y. T., Rudd, E., Zheng, C., Edner, J., Ma, D., Wood, S. M., Bechensteen, A. G., Boelens, J. J., Celkan, T., Farah, R. A., Hultenby, K., Winiarski, J., Roche, P. A., Nordenskjold, M., Henter, J. I., Long, E. O. and Ljunggren, H. G. (2007) Defective cytotoxic lymphocyte degranulation in syntaxin-11-deficient familial hemophagocytic lymphohistiocytosis 4 (FHL4) patients. Blood

43 D'Andrea-Merrins, M., Chang, L., Lam, A. D., Ernst, S. A. and Stuenkel, E. L. (2007) Munc18c interaction with syntaxin 4 monomers and SNARE complex intermediates in GLUT4 vesicle trafficking. J. Biol. Chem. **282**, 16553-66

44 Richmond, J. E., Weimer, R. M. and Jorgensen, E. M. (2001) An open form of syntaxin bypasses the requirement for UNC-13 in vesicle priming. Nature **412**, 338-41

45 Hammarlund, M., Palfreyman, M. T., Watanabe, S., Olsen, S. and Jorgensen, E. M. (2007) Open syntaxin docks synaptic vesicles. PLoS Biol. **5**, e198

46 van Weering, J. R., Toonen, R. F. and Verhage, M. (2007) The role of Rab3a in secretory vesicle docking requires association/dissociation of guanidine phosphates and Munc18-1. PLoS ONE **2**, e616

47 Gulyas-Kovacs, A., de Wit, H., Milosevic, I., Kochubey, O., Toonen, R., Klingauf, J., Verhage, M. and Sorensen, J. B. (2007) Munc18-1: sequential interactions with the fusion machinery stimulate vesicle docking and priming. J. Neurosci. **27**, 8676-86

48 Connell, E., Darios, F., Broersen, K., Gatsby, N., Peak-Chew, S. Y., Rickman, C. and Davletov, B. (2007) Mechanism of arachidonic acid action on syntaxin-Munc18. EMBO Rep. **8**, 414-9

## Figure legends

**Figure 1. Syntaxin 1 is *S*-nitrosylated**

*S*-nitrosylation of brain lysate proteins by NO donors was detected as a decrease in biotinylation of protein cysteine residues using the biotin loss assay.

**(A) and (B)**, Biotinylated proteins were affinity purified from lysate treated with 1 mM GSNO using neutravidin-sepharose and detected by avidin overlay **(A)** or western blotting **(B)**. Reduced amounts of syntaxin 1 and SNAP-25 were recovered, indicative of *S*-nitrosylation

**(C)** Syntaxin 1 immunoprecipitated from brain lysate treated with 1 mM NOR-1 showed less biotinylation, indicative of direct *S*-nitrosylation.

**Figure 2. Syntaxin 1 *S*-nitrosylation inhibits Mode 1 binding to Munc18-1**

**(A) and (B)** GST-syntaxin 1a pre-bound to glutathione-coated beads was treated with 1 mM NOR-1 or NEM and incubated with brain lysate (*pre-assembly*); or alternatively, incubated with brain lysate and subsequently treated with NOR-1 or NEM (*post-assembly*). Bound proteins were separated by SDS-PAGE and detected by Coomassie blue stain **(A)** or western blotting **(B)**.

**(C)** GST-syntaxin 1a pre-bound to glutathione coated plates was treated with 1 mM NOR-1 or NEM, washed and then incubated with $^{35}$S-labelled Munc18-1. Bound Munc18-1 was measured by scintillation counting.

**(D)** GST-syntaxin 1a pre-bound to glutathione coated plates was either left untreated, or treated with 1 mM NEM before being incubated with His-SNAP-25 (*SYX+NEM*); or alternatively, incubated with SNAP-25 that had been pre-treated with 1mM NEM (*SNAP-25+NEM*). Bound SNAP-25 was detected by ELISA.

**(E)** GST-syntaxin 1a pre-bound to glutathione coated plates was treated with increasing concentrations of NOR-1 or SIN-1 before incubation with $^{35}$S-labelled Munc18-1. Bound Munc18-1 was measured by scintillation counting. The amount of NO released by each concentration of donor was assayed in parallel using a Griess assay.

Data are shown as mean ± S.E.M.

**Figure 3. NO does not inhibit binding of Munc18-1 to the SNARE complex**

**(A)** GST or GST-complexin pre-bound to glutathione-coated beads was incubated with brain lysate, in the presence or absence of 1 mM NEM, and bound proteins detected by western blotting. Treatment with NEM had no effect on SNARE complex co-precipitation, but inhibited Munc18-1 binding,.

**(B)** GST-complexin pre-bound to glutathione-coated beads was incubated with brain lysate in a 2-stage protocol. In stage 1, all samples were incubated with brain lysate, either untreated (*control*) or in the presence of 1 mM NOR-3 or NEM. After washing, samples were either eluted (-) or alternatively subjected to a second incubation with brain lysate in the presence or absence of 1 mM NOR-3 or NEM (Stage 2). NEM inhibits Munc18-1 co-precipitation with the SNARE complex (lanes 2 & 4) but not the capacity of the SNARE complex to interact with Munc18-1 when NEM is washed away (lane 6); whereas NOR-3 has no effect.

**Figure 4. *S*-nitrosylation of syntaxin 1a at Cys145: evolutionary conservation and structural predictions.**
**(A)** Sequence alignment of syntaxins, highlighting Cys145 in human syntaxin 1a.
**(B)** *Upper panels*: (*left*) Structure of Munc18-1 (yellow) bound to syntaxin 1a (blue) in the closed conformation (pdb entry: 1dn1). Cys145, (red spheres), is not part of the binding interface with Munc18-1. (*right*) Close-up of the interaction between Cys145 (red spheres) in the Hc helix with Ile202 (blue spheres) in the H3a region of the SNARE helix. *Lower panels*: (*left*) Molecular dynamics simulation of wild type (blue) and *S*-nitroso-Cys145-modified (cyan) syntaxin 1a, using atomic coordinates from the 1dn1 crystal structure. Stable average structures are superimposed, with *S*-nitroso-Cys145 shown in red spheres. Cys145 nitrosylation results in movement of the linker region that connects Hc to the H3 SNARE helix, and also alters the orientation of the C-terminal H3c helix (see arrows). (*right*) Molecular dynamics simulation of wild type (blue) and C145W mutant syntaxin 1a (purple, with Trp145 in red spheres). The mutation affects the packing of the H3 SNARE helix against the Hc helix, altering the local structure of the nearby linker region and also the C-terminal H3c helix (see arrows), similar to the effects of the *S*-nitrosocysteine modification.

**Figure 5. Nitrosomimetic syntaxin mutants C145M and C145W show reduced Mode 1 binding to Munc18-1.**
**(A)** Recombinant wild type and C145W mutant syntaxin 1a, and NSF, were subjected to the biotin loss assay in the presence or absence of 1 mM GSNO. Samples were run on SDS-PAGE and detected by immunoblotting (*left panel*) or avidin overlay (*right panel*). Wild type syntaxin and NSF showed NO-inhibitable biotinylation, indicative of direct *S*-nitrosylation. In contrast, C145W exhibited negligible biotin labelling, suggesting that C145 is the *S*-nitrosylation site in syntaxin 1a.
**(B)** GST-tagged wild type and mutant syntaxins pre-bound to glutathione coated beads were treated with 1mM NEM or NOR-1 before incubation with brain lysate. Bound proteins were separated by SDS-PAGE and detected using Coomassie blue stain. C145M, C145W and open mutant syntaxins all show reduced Munc18-1 binding, similar to that seen when wild type GST-syntaxin is pre-incubated with 1mM NEM or NOR-1. C145S syntaxin is insensitive to NO or NEM pre-treatment.
**(C)** GST-tagged wild type and mutant syntaxins or GST pre-bound to glutathione coated plates were incubated with $^{35}$S-labelled Munc18-1. Bound Munc18-1 determined by scintillation counting was reduced in C145M, C145W and open mutant syntaxins, but not C145S.
**(D)** All of the GST-tagged proteins showed equivalent binding to his-SNAP-25, as determined by ELISA.
**(E)** The GST-tag was removed from wild type syntaxin and the nitrosomimetic C145M and C145W mutants using thrombin. These proteins were then analysed by CD spectroscopy.
Binding data are shown as mean ± S.E.M

**Figure 6. Munc18-1 colocalisation with syntaxin 1a in live cells is dependent on Cys145.**
**(A)** Wild-type or mutant mCerulean-Syntaxin 1a ($Syx_{1\text{-}288}$, *green*), and EYFP-Munc18-1 (Munc18-1, *red*) were expressed in N2a cells and imaged by confocal laser scanning microscopy. The 2-D histogram represents the intensity for each channel in each voxel with a colour scale representing frequency. The residual map indicates fluorescence channel covariance. The hue is from -1 to 1 with *cyan* corresponding to a

zero residual. Note the Munc18 redistribution and intracellular purple hue in the NEM-treated wild type $Syx_{1-288}$ and the C145W samples, indicating a lack of syntaxin-Munc18-1 co-localisation. Scale bar: 5 µm, except for EYFP control (2 µm). **(B)** Combined covariance analysis of mCerulean-Syntaxin 1a and EYFP-Munc18-1. Pearson's correlation coefficients are shown as mean ± S.E.M (n>4 cells per condition). ** $P < 0.002$ compared to $Syx_{1-288}$.

**Figure 7. Modification of syntaxin 1a at Cys145 disrupts interaction with Munc18-1 in living cells.**

**(A)** In the absence of an energy acceptor (*top panels*) mCerulean-$Syx_{1-288}$ traffics efficiently to the cell surface (intensity image, *left panel*). The excited state fluorescence decay of the donor was mono-exponential, exhibiting a single, long fluorescence lifetime of 2288 ± 40 ps (blue hue in FLIM, *right panel*). When co-expressed with the EYFP-Munc18-1 FRET acceptor, bi-exponential fluorescence decay of $Syx_{1-288}$ was exhibited, with a reduction in overall fluorescence lifetime due to FRET (note yellow/green hues in FLIM map). Treatment of $Syx_{1-288}$ with 1 mM NEM abolished detectable interaction with Munc18-1 on the cell surface (blue hue, similar to that seen in the absence of Munc18-1). In contrast, Munc18-1 interaction was not abolished with $Syx_{1-288}$ [C145W] or by identical NEM treatment of $Syx_{1-288}$ [C145S] (green/yellow hues).

**(B)** Quantification of fluorescence lifetimes. Data are shown as mean ± S.E.M (n=3 cells per condition). ** $P < 0.002$ compared to $Syx_{1-288}$.

**Figure 8. Nitrosomimetic syntaxin C145W alters exocytosis kinetics and increases quantal size.**

Chromaffin cells were co-transfected with EGFP and syntaxin 1a mutants and amperometric recordings taken after permeabilization/stimulation with digitonin/$Ca^{2+}$.

**(A)** Overexpression of C145W slowed secretory granule release kinetics and increased quantal size. Data are shown as mean ± S.E.M. for untransfected (n = 735 spikes), C145S (n = 162 spikes), C145W (n = 249 spikes) and open (n = 169 spikes). * $P<0.03$, ** $P<0.001$ compared to untransfected.

(**B**) Transfection of HeLa cells with C145S, C145W or open syntaxin constructs indicated that they were all expressed at similar levels.

Biochemical Journal Immediate Publication. Published on 02 May 2008 as manuscript BJ20080069

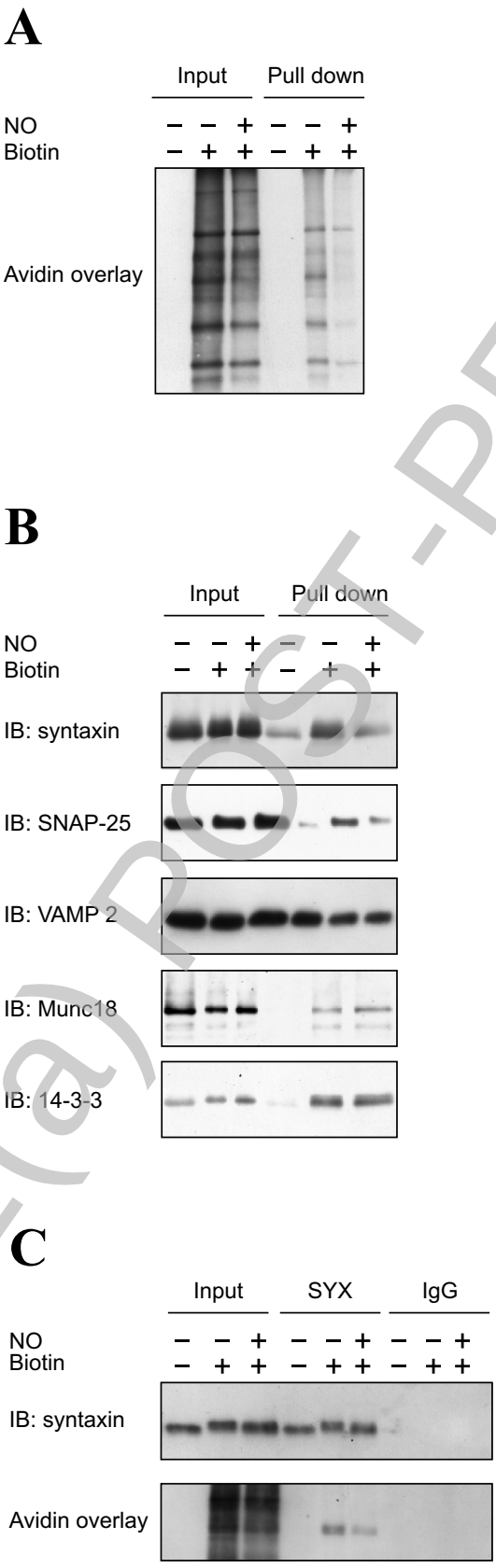


Figure 1. Palmer et al

Biochemical Journal Immediate Publication. Published on 02 May 2008 as manuscript BJ20080069

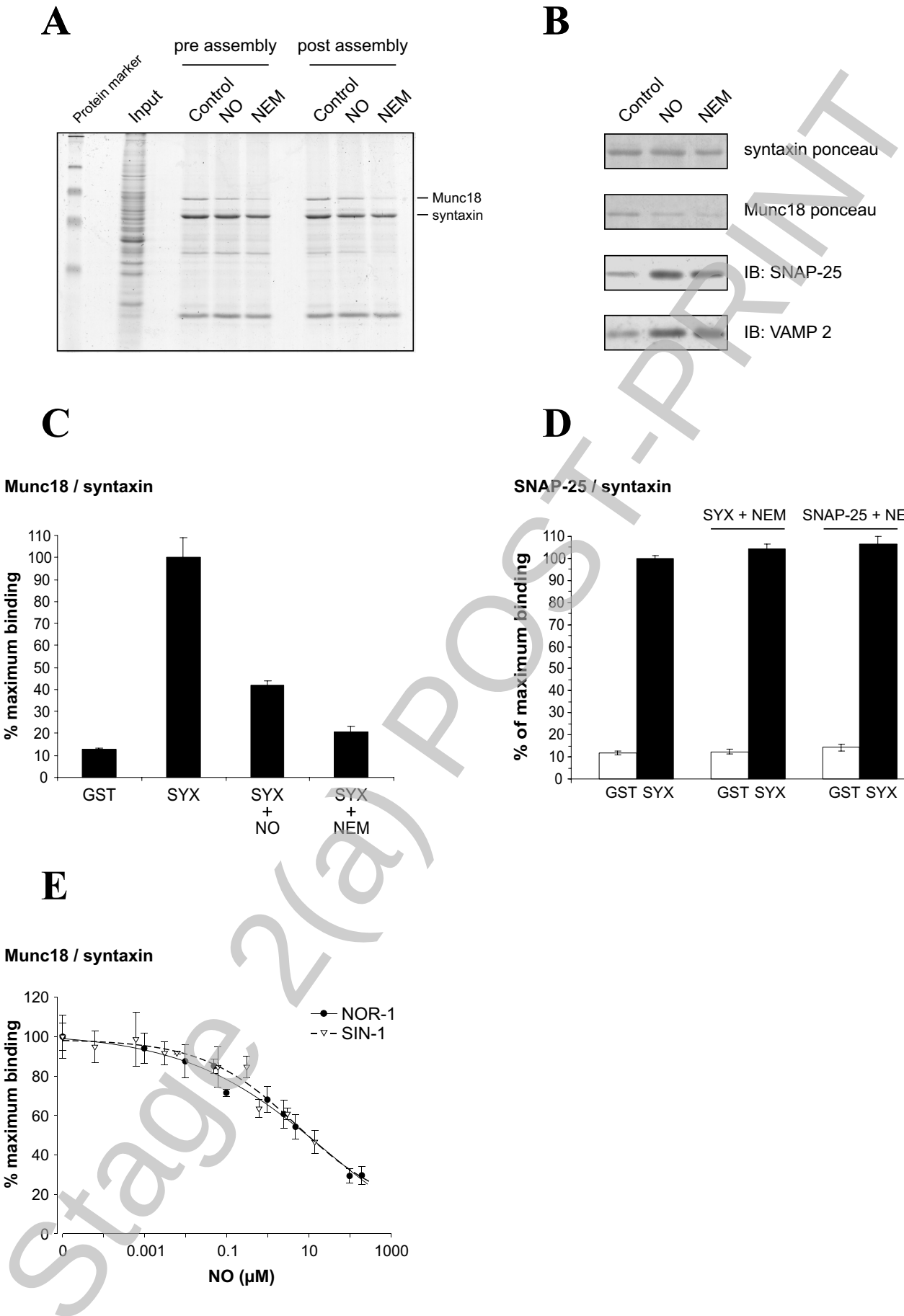


Figure 2. Palmer et al

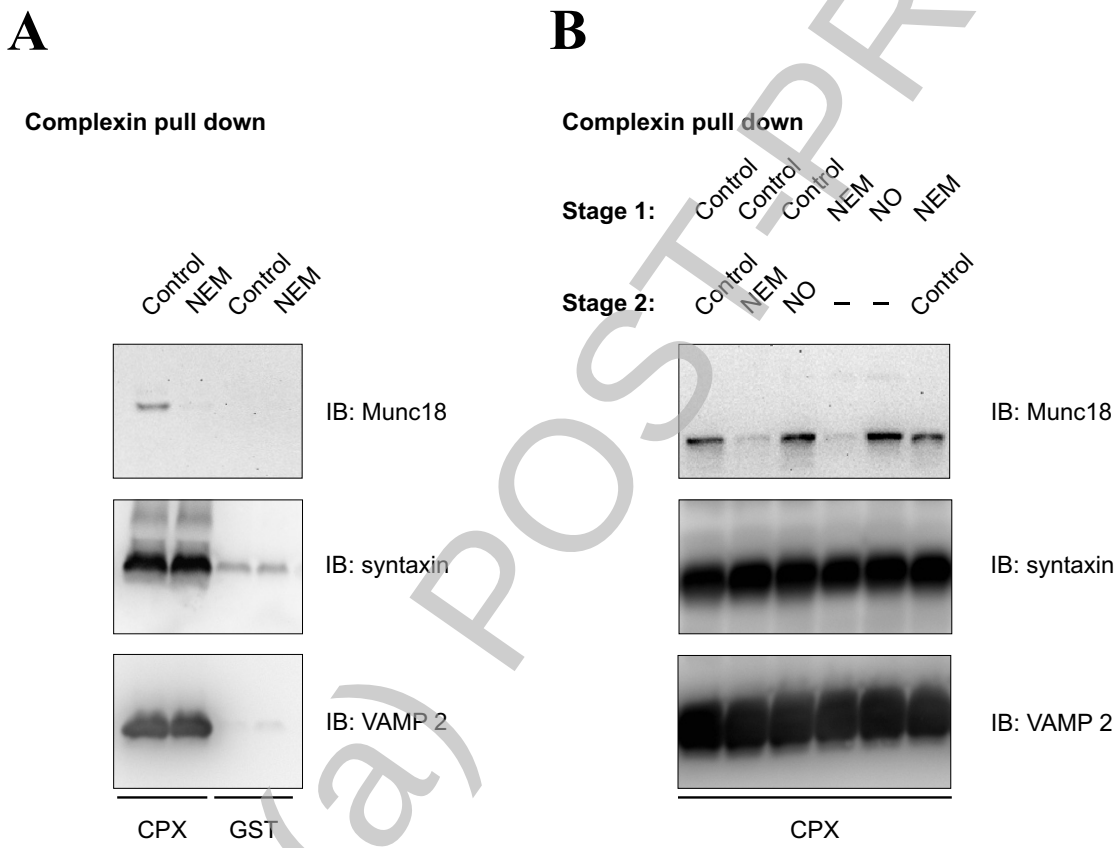


Figure 3. Palmer et al

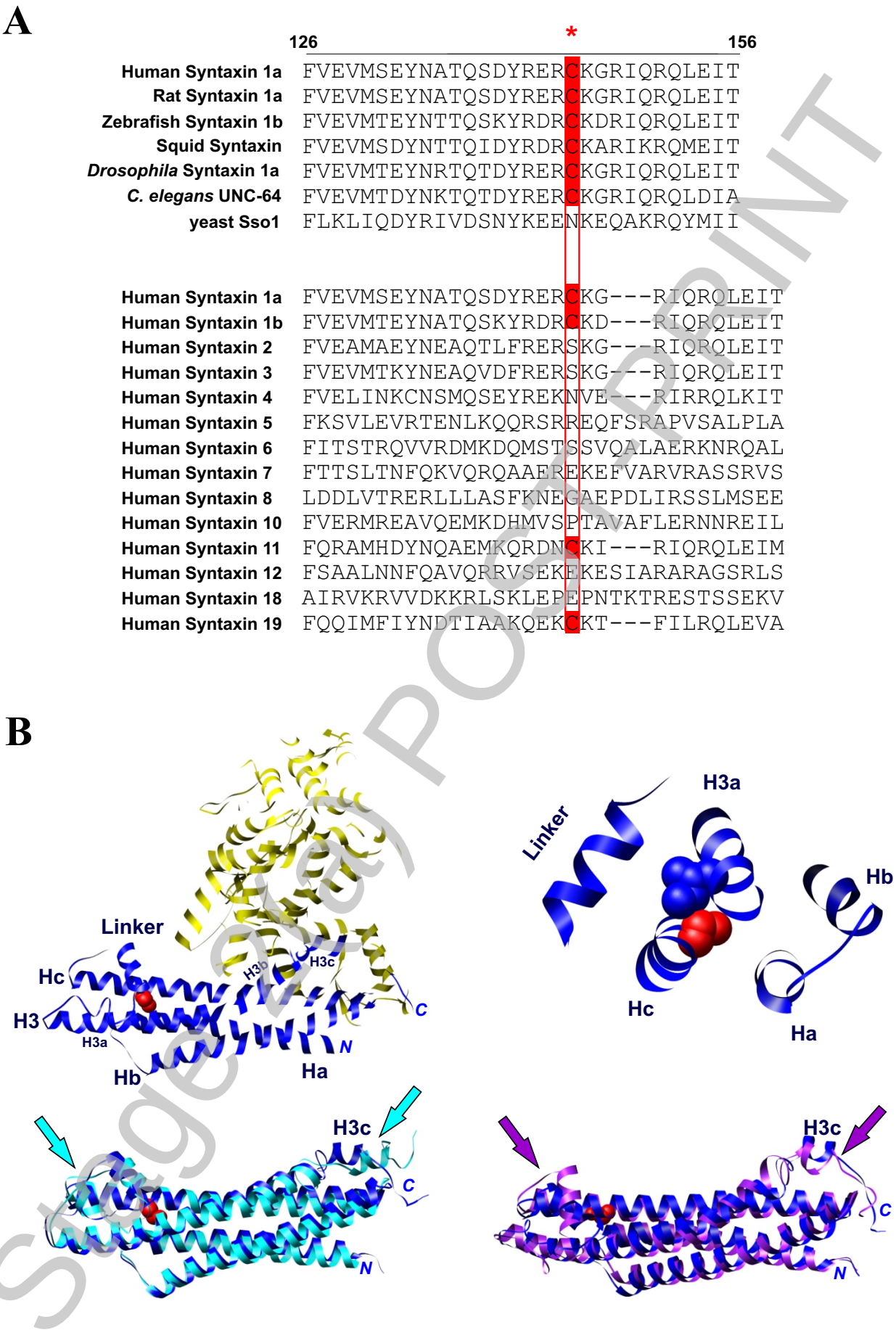


Figure 4. Palmer et al

Biochemical Journal Immediate Publication. Published on 02 May 2008 as manuscript BJ20080069

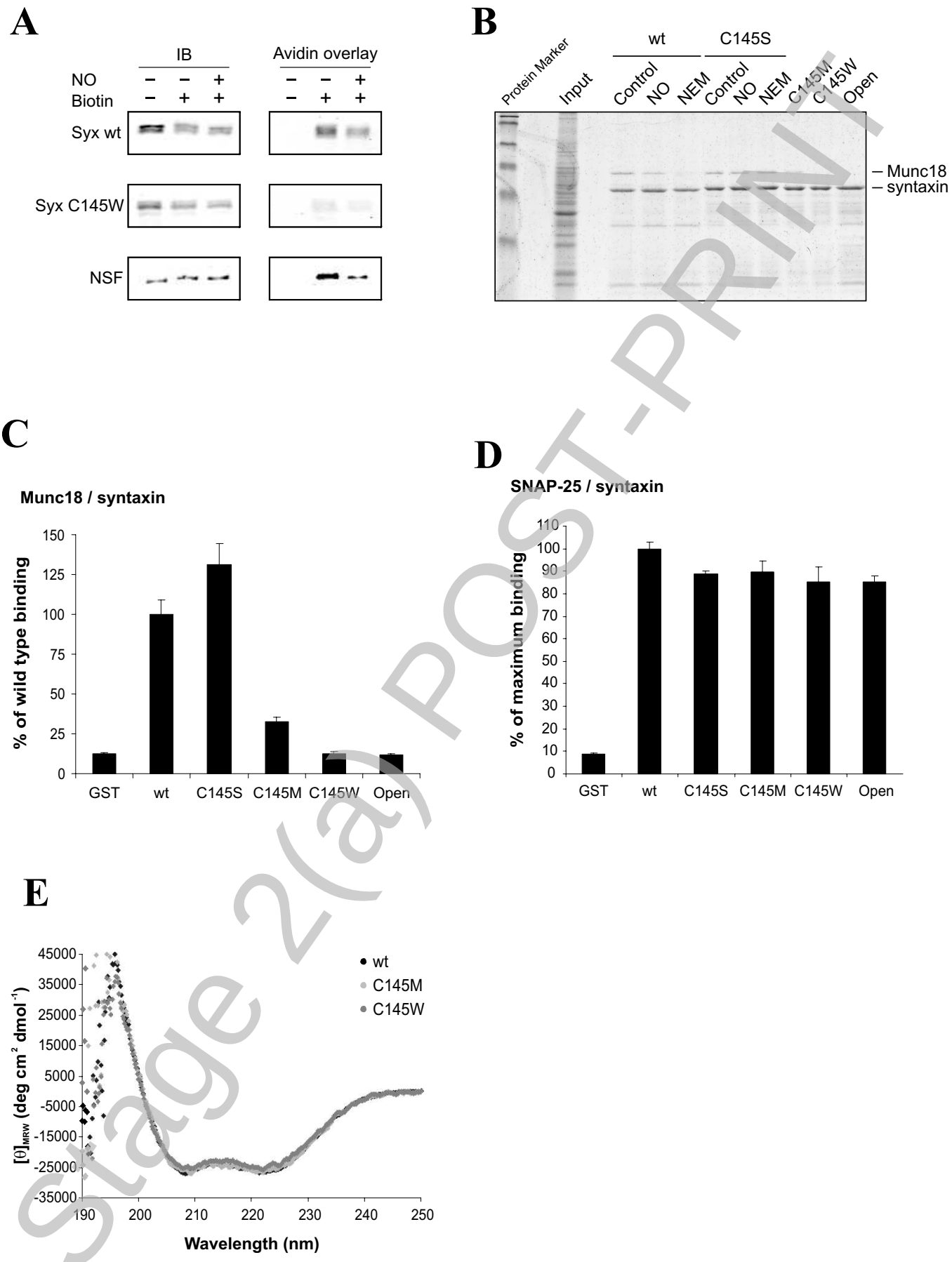


Figure 5. Palmer et al

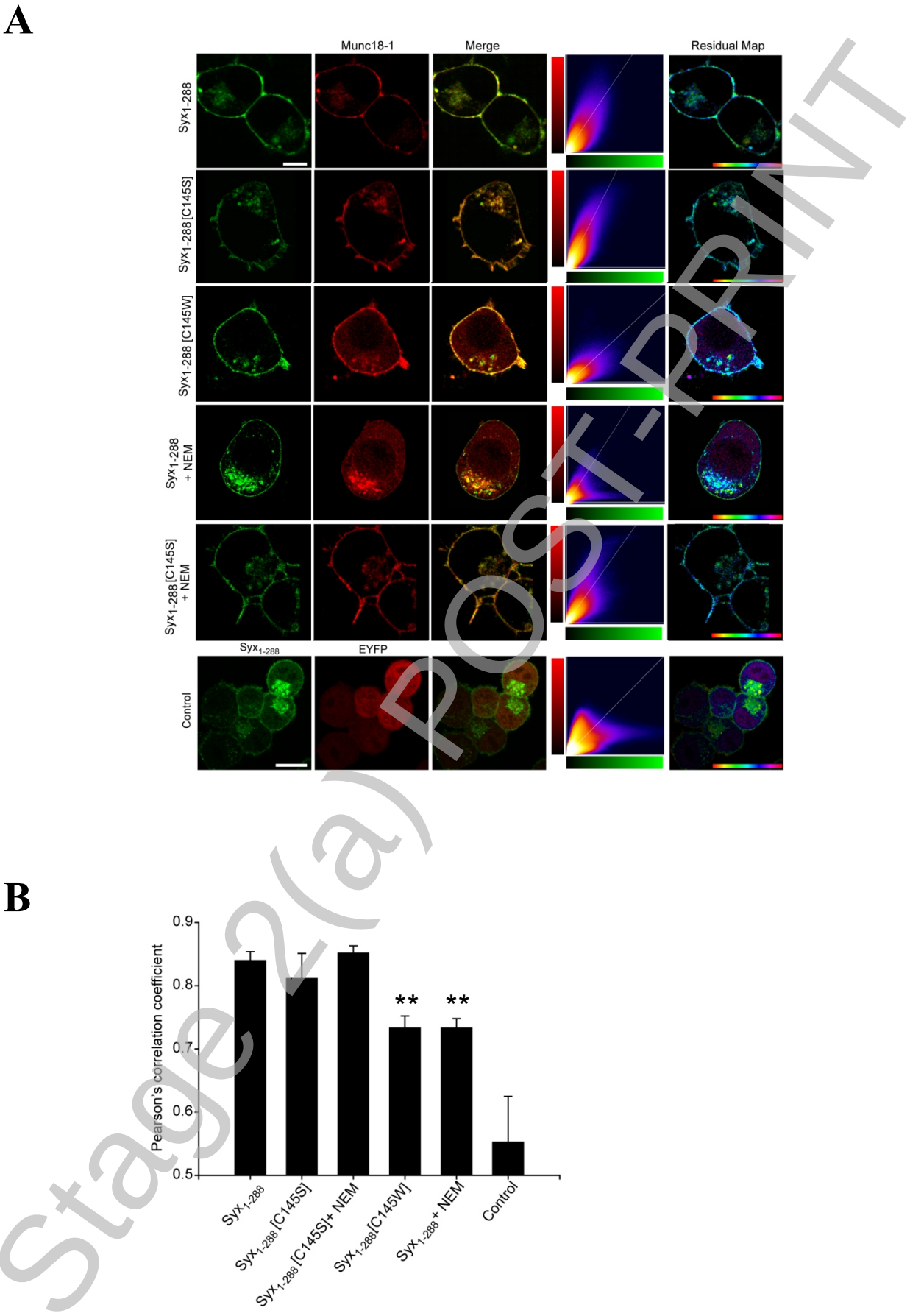


Figure 6. Palmer et al

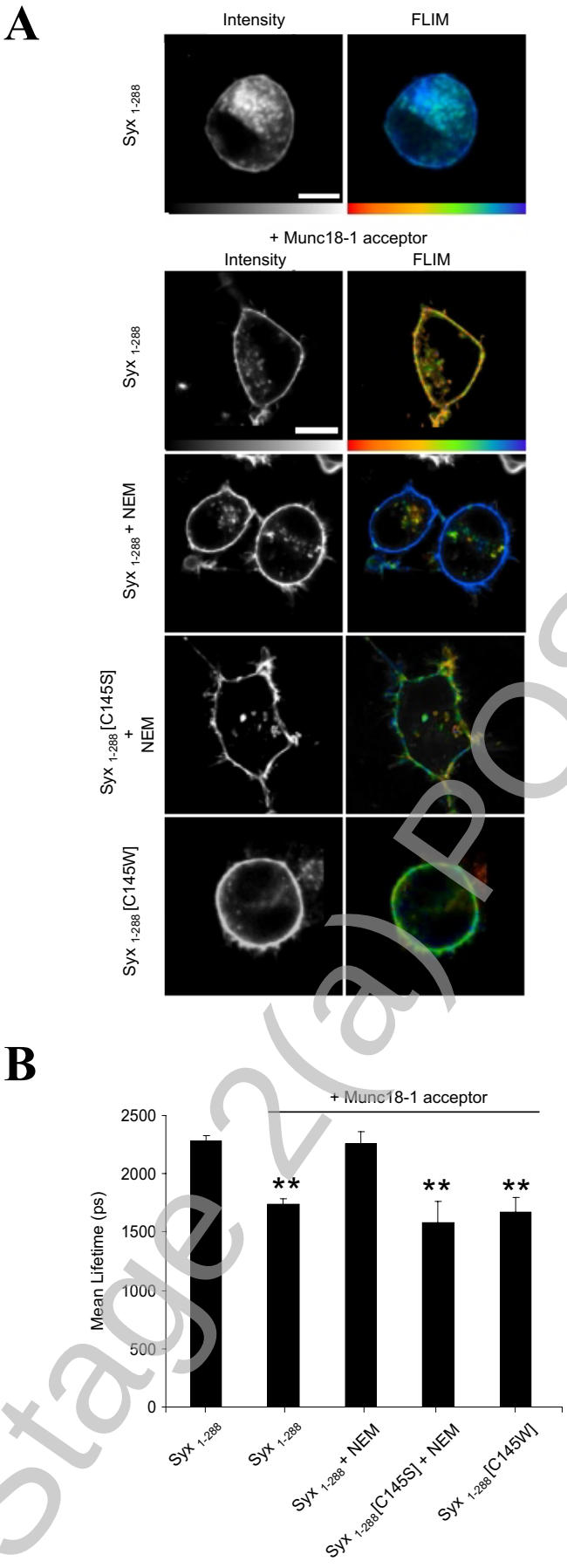


Figure 7. Palmer et al

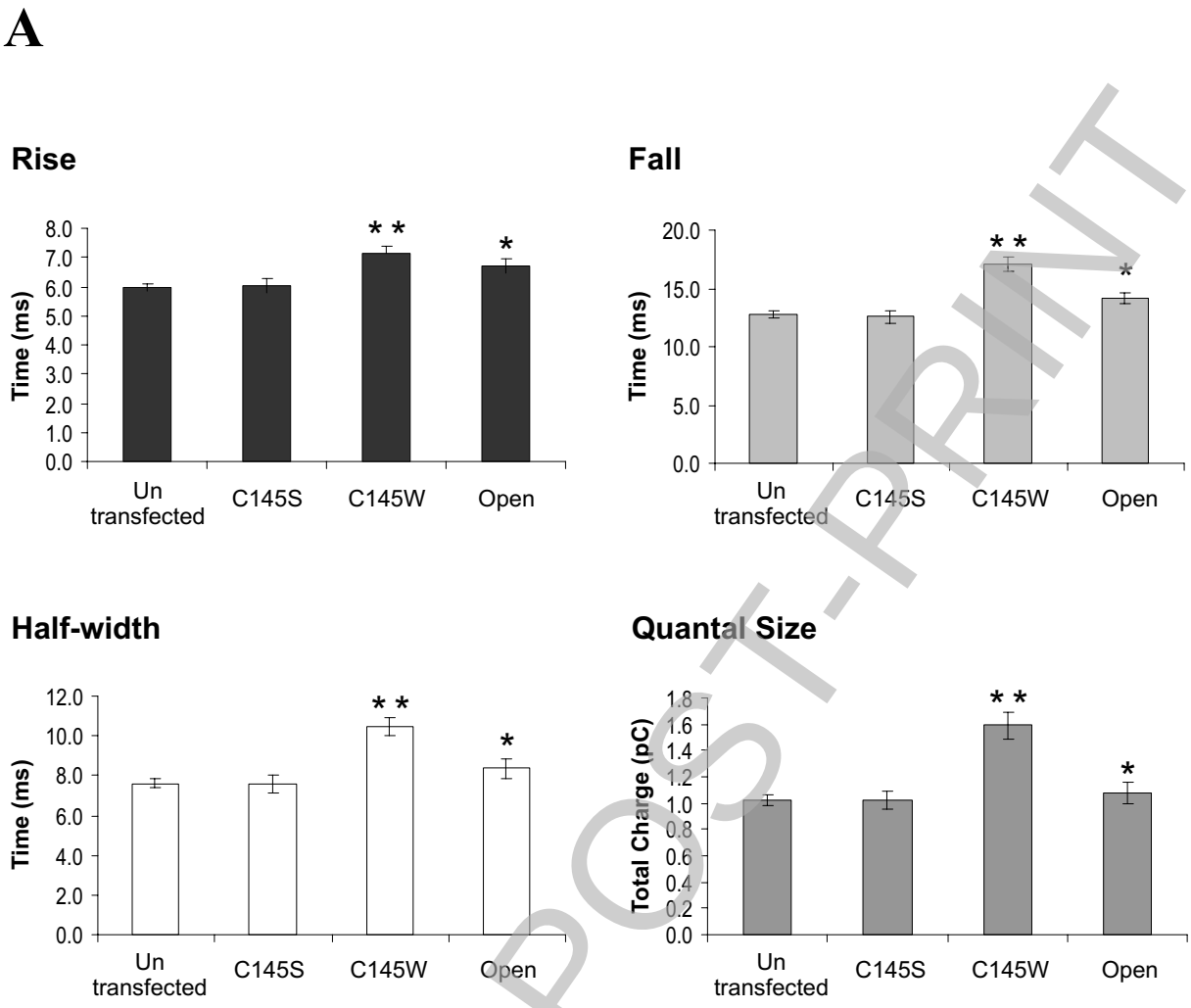


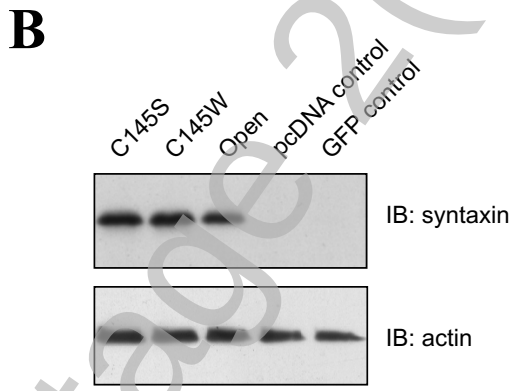


Figure 8. Palmer et al